ARID ZONE JOURNAL OF ENGINEERING, TECHNOLOGY & ENVIRONMENT
AZOJETE December 2019. Vol. 15(4):1049-1060
Published by the Faculty of Engineering, University of Maiduguri, Maiduguri, Nigeria.
Print ISSN: 1596-2490, Electronic ISSN: 2545-5818
www.azojete.com.ng

ORIGINAL RESEARCH ARTICLE

DEVELOPMENT OF A PSEUDO-CLOSED LOOP SOLAR COLLECTOR SUN TRACKING SYSTEM WITH OPTIMIZED SET-POINT PATHS FOR FLAT PLATE PAYLOAD

M. T. Jimoh* and A. B. Aliyu

(Department of Mechanical Engineering, Bayero University, Kano, Nigeria)
** Corresponding author's email address: mtjimoh.mec@buk.edu.ng*

ARTICLE INFORMATION

Submitted 31 January, 2019
Revised 07 July, 2019
Accepted 07 July, 2019

Keywords:
Solar collector
solar tracking
closed-loop tracking
open-loop tracking
angle of incidence.

ABSTRACT

This paper provides the theoretical framework for the development of a pseudo-closed loop solar tracking system incorporating a microcontroller for a flat payload, where the outputs of the system (the slope and the azimuth angles of the payload) are observed and the set-points for the system are to be optimally computed by the microcontroller. It also presents, from literature, the equations and models solar angles and incident angles for the development of the optimum set point path for the tracking, and gives the outline of the signal flow plan, as well as the corresponding flowchart, for the tracking system's components interaction. The concept would provide a cheaper and simpler alternative to dual axis solar tracking incorporating solar sensors. The models presented here are adaptable to any geographical location in Nigeria and globally.

1.0 Introduction

Conventional energy sources like oil and coal still constitute more than 80% of the global energy mix (IEA, 2018). Yet apart from being finite, the conventional energy sources pollute and warm the environment. According to a report by (NASA, 2018), about 97% of actively publishing climate scientists agree that the earth's climate is warming due to human activities, especially the use of fossil fuels. These reasons have given impetus to the exploration and use of non-conventional, clean, and renewable energy sources such as solar energy and wind energy. Solar energy is the direct utilization of the sun's radiant energy.

A major component of all solar energy applications is the payload - the part that absorbs the solar energy directly and converts it to a useful form, or transmits it to another media. In helio-electrical applications, the payload is the solar photo-voltaic panel, and it is a solar collector in helio-thermal applications. Solar collectors absorb solar energy and convert it into heat which is then transferred to a stream of liquid or gas. To get the most from solar payloads, they must be pointed to the directions that capture the most solar energy. In general, results show that solar tracking can increase the yearly energy capture by up to 40% compared to the case in which the payload is fixed (Bari, 2000, Lee et al., 2009, Mohd et al., 2001).

Solar tracking can be manual or automatic. In automatic solar tracking, the payload tracks the sun at all times with very little human intervention (that is the angle of incidence of the sun with respect to the receiving surface of the payload equal to zero at specified times). In the strict sense, there are two categories: open loop tracking and closed loop tracking. Between these two categories, there can be another – a pseudo closed loop solar tracking. All these are explained as follows.

1.1 Open loop solar tracking

In open-loop tracking, data of the desired payload's altitude and surface azimuth angles at specified times are computed based on some sun-earth geometry or models, or solar irradiation algorithms. The data is fed into, or computed by, an appropriately coded microcontroller which, using information from a real time clock sends signal to an actuating mechanism to manipulate the altitude and surface azimuth angles of the payload appropriately. Figure 1 gives a schematic of a general open-loop solar tracking. It can be seen from the figure that an open-loop solar tracking system only manipulates the altitude and/or surface azimuth angles of the payload, it does not observe the actual payload's incidence angle using any form of sensor or feedback mechanism, so it cannot correct for any errors in the actual incidence angle. For this reason, it is poor in disturbances rejection.

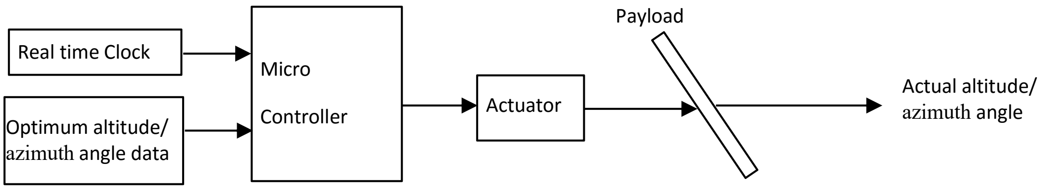

Figure 1: Schematic of open loop solar tracking

Models and algorithms for computing the desired paths for open-loop solar tracking systems exist in literature. Some of these modes and algorithms require basic input parameters such as date, time (local standard time (LST), time zone (TZ)), longitude, latitude and surface azimuth rotation of a location. The very complex and precise algorithms are contained in Blanco-Muriel et al. (2001), Michalsky (1988), Grena (2008), Meeus (1998) and Reda and Andreas (2004). Actual development or design and construction of open loop solar trackers using a form of the formulas and algorithms already mentioned have also been reported. Among them is Al-Naima and Yaghobian (1990), who designed and constructed a dual axis sun tracker in which the controller is a microprocessor. Abdallah and Nijmeh (2004) used PLC controllers in the dual sun tracker they developed.

1.2 Closed loop solar tracking

Closed-loop tracking systems are based on feedback control principles. In these systems, the payload's incident angle is sensed indirectly through a system of light detecting or measuring devices such as light detecting resistors (LDR), pyrheliometer and four quadrant photo detectors. Using feedback mechanisms, the error signal from the sensed incident angles are sent to a controller, which carries the necessary control action and send to the actuator. A form of closed-loop tracking system (with provision for alternate set point input) is shown in Figure 2. Because of the light sensor and controllers required in their operations, closed loop solar tracking systems are generally more complicated and expensive than the open-loop solar tracking systems.

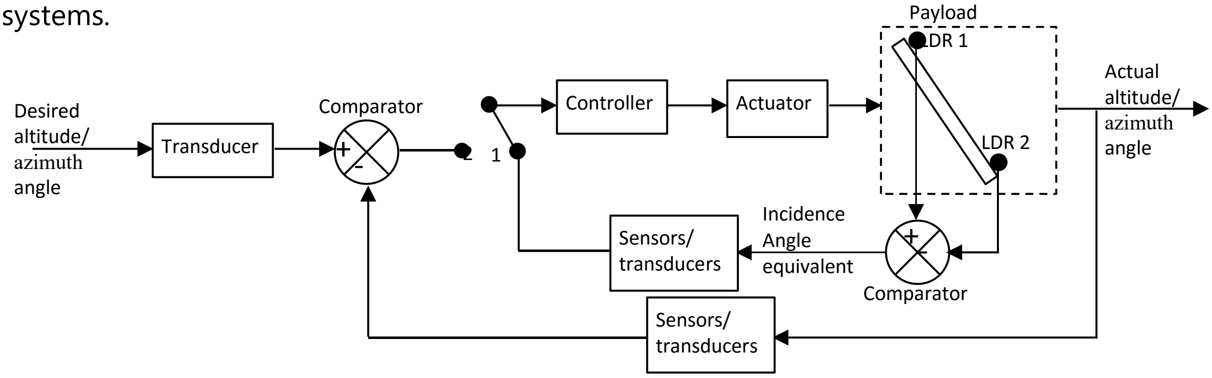

Figure 2: Schematic of closed loop solar tracking

Corresponding author's e-mail address: mtjimoh.mec@buk.edu.ng

Different types of closed loop solar tracking systems have been developed. Kalogirou (1996), Barsoum (2011) and Aiuchi et al. (2004) employed light-dependent resistors (LDRs) in their one-axis closed loop solar tracking systems. Jiang and Cao (2003) used an emulated sunflower based on a spherical four-quadrant photoelectric sensor for sensing the incident angle of their solar tracking systems. Roth et al. (2004) and Georgiev et al. (2004) designed and constructed a sun tracking system in which a pyrheliometer was used to measure the direct solar radiation, a four-quadrant photo detector to sense the sun's position. Xinhonz et al. (2007) and Alata et al. (2005) used fuzzy logic algorithms in their controllers.

The objective of this paper is to develop a tracking system that is a bridge between the open loop system and closed loop system described above. Such developed tracking system is termed pseudo-closed loop solar tracking system and the process is presented in the following Section.

2.0 Materials and Methods

The main material for this research is a computing facility with MATLAB® software. The methods include conceptualising the pseudo-closed loop solar tracking system, presenting and simulating the solar energy equations required for developing the optimum set points for the pseudo tracking system, and developing the procedure required for implementing the pseudo closed loop solar tracking system.

2.1. The pseudo-closed loop solar tracker concept

The proposed pseudo-closed loop solar tracker will have all the features of an open loop system but would also incorporate a feedback system to observe the altitude and surface azimuth angles of the payload. It is a pseudo-closed loop tracker in the sense that the feedback would not observe the actual incidence angle of the sun. The development of the concept of the tracker, and its components, as well as the development of the equations to be used for obtaining its optimum set-points, and its signal flow plan, are presented in the following sub-Sections.

Figure 3 is a schematic of the pseudo-closed loop solar tracker. Compared to a closed loop system of the type shown in Figure 2, the pseudo-closed loop system would use a smaller number of sensors/transducers, and would avoid the use of controllers like PID, Fuzzy logic and the like, that may introduce additional complications in design and implementation. It has as its major components a microcontroller, a real time clock, angular position sensors and actuators. The microcontroller uses signal from the real time clock to determine which value from the optimum altitude and azimuth data set to be used as error signal for the actuator at specified time interval. The optimum dataset may be supplied externally, as indicated in Figure 3, or the codes for generating it may be stored in the microcontroller and the optimum dataset computed

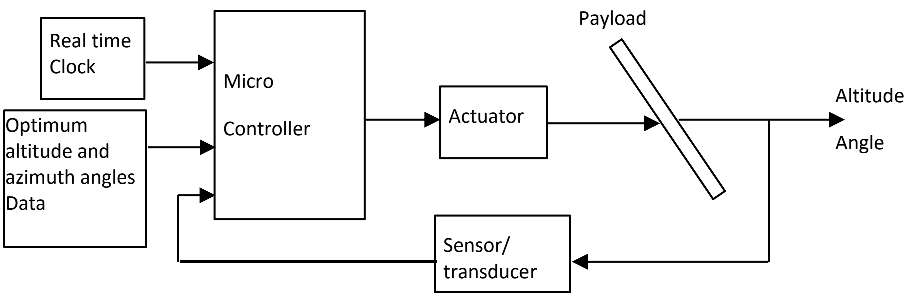

Figure 3: Schematic of pseudo-closed loop solar tracking system

This concept does not correct for any errors in the actual incidence angles: this will depend on the accuracy of the algorithm used to obtain the optimum set point paths, and the system set-up and calibration during installation. In addition, having optimized set-point calculation incorporated in a pseudo-closed loop system is an avenue to experiment on the correctness of existing solar angle models and algorithms.

2.2 Developing the Optimum set point path for the pseudo-closed loop solar tracker

The main aim of solar tracking is always to try and keep the angle of incidence of solar radiation on a payload at or close to zero . Optimum set point path is about being able to specify the degree of vertical and/or horizontal rotation of the payload necessary to make the angle equal to zero at specified times. For this a form of solar geometry formulas or algorithms for estimating the angle of incidence and the position of the sun, is required.

For many solar energy applications, tracking accuracy of between 0.1° and 0.25° is sufficient given that the diameter of the solar disk subtends an angle of 0.52° (at aphelion, when the sun is farthest) to 0.54° (at perihelion, when the sun is closest) in the sky (Myer, 2013). For these situations, solar tracking equations or algorithms used need not be overly complex. The basic equations for estimating the angle of incidence as contained in Duffie and Beckman (1991), Tiwari (2002), Myer (2013), and some solar energy books as described in this section will suffice for those situations.

2.2.1 Angle of incidence (θ_i)

For a flat payload, the angle of incidence (θ_i) is the angle between the beam radiation and the normal to the surface of the payload (Duffie and Bechman, 1991). This angle is a function of three sun-earth angles - the latitude angle (ϕ), the declination angle (δ), the hour angle (ω), and two other angles which define the placement of the payload on a surface – its slope angle (β) and its surface azimuth angle (γ). The geometrical relationships between these angles are shown in Figure 4. The angle of incidence is defined by its cosine (Duffie and Beckman, 1991) as:

$$\cos\theta_i = \sin\delta\sin\phi\cos\beta + \cos\delta\cos\phi\cos\beta\cos\omega + \cos\delta\sin\phi\sin\beta\cos\gamma\cos\omega + \cos\delta\sin\beta\sin\gamma\sin\omega - \sin\delta\cos\phi\sin\beta\cos\gamma \quad (1)$$

The latitude angle, together with the longitude angle, uniquely defines a location on the earth's surface. The declination angle and the hour angle are defined as follows:

a) Declination angle (δ)

The declination angle is the angle between the equatorial plane and a line joining the centres of the Sun and the Earth, and this angle gives rise to variation in the length of the day (sunshine hours) throughout the year. The equation for calculating the declination angle for a non-leap year is given (Duffie and Beckman, 1991) as:

$$\delta = 23.45\sin\left[\left(\frac{360}{365.25}\right)(284 + n)\right] \quad (2)$$

where n is the number that represents the day of the year, for example, n = 32 on the 1st of February.

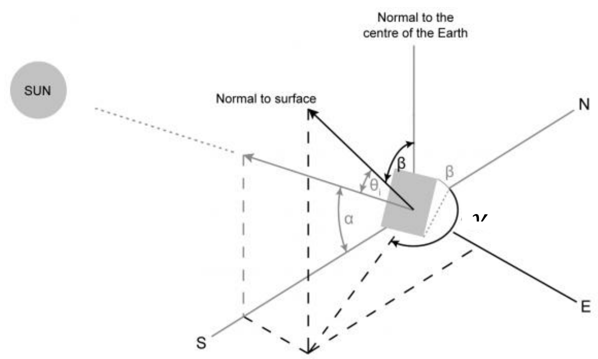

Figure 4: Relationship between Azimuth, Zenith, Altitude and Incidence angles

b) The Hour angle (ω)

The hour angle is the angle of the sun from Solar Noon. For solar radiation calculations, the solar time is used instead of the local standard time. When the solar time (ST) for the location in hours is known, the hour angle can be calculated from (Tiwari, 2002):

$$\omega = 15(\mathrm{ST} - 12) \quad (3)$$

While the local standard time (LST) is always known, the solar time (ST) for a location is obtained from calculation as (Iqbal, 1983):

$$\mathrm{ST} = \mathrm{LST} - 4(\psi_{st} - \psi_a) + \mathrm{ET} \quad (4)$$

where,

ψ_{st} = the standard longitude (time zone), in degrees, for the location.

ψ_a = the actual longitude angle (in degrees) for the location.

LST = the local standard time (in hours)

and ET is the equation of time in hours given as (Spencer, 1971):

$$\mathrm{ET} = \left(\frac{229.2}{60}\right)(0.000075 + 0.001868\cos B - 0.032077\sin B - 0.014615\cos 2B - 0.04089\sin 2B) \quad (5)$$

where B is defined as:

$$\mathrm{B} = 360(\mathrm{n} - 1)/365 \quad (6)$$

2.2.2 The position of the sun

The position of the sun with respect to a location on the earth's surface can be defined using the altitude angle (α), the Zenith angle (θ_Z) as well as the solar azimuth angle (γ_s). The relationships between these angles are defined as follows:

a) Altitude angle and Zenith angle

The zenith angle is the angle between the sun's ray and the perpendicular line to a horizontal plane at the location (Figure 7). The altitude angle (α) is the complement of the zenith angle. The altitude angle (and the zenith angle) can be calculated from the expression (Myer, 2013):

$$\sin\alpha = \cos\theta_Z = \sin\delta\sin\phi + \cos\delta\cos\omega\cos\phi \quad (7)$$

b) The solar azimuth angle (γ_s)

In the northern hemisphere, the solar azimuth angle is the angle between the projection on a horizontal plane, of a line between the sun and a point (say P), and the line due South (Figure 4). In the southern hemisphere, it is defined as the angle between the projection and the line due north. By convention, the azimuth angle is taken as negative East of South and positive West of South for northern hemisphere (it is taken as negative East of North and positive West of North for southern hemisphere). This means that γ_s is negative in the morning, and positive in the afternoon, and therefore, the sign of γ_s should match that of the hour angle ω. The solar azimuth angle can be calculated from the expression (Myer, 2013):

$$\cos\gamma_s = (\sin\alpha\sin\phi - \sin\delta)/(\cos\delta\cos\phi) \quad (8a)$$

or

$$\cos\gamma_s = (\cos\delta\sin\phi\cos\omega - \sin\delta\cos\phi)/\cos\alpha = (\cos\delta\sin\phi\cos\omega - \sin\delta\cos\phi)/\sin\theta_z \quad (8b)$$

Taking the inverse cosine to obtain γ_s in Equation (8) will not always come with the correct sign. So, it must be ensured that γ_s takes the sign of the hour angle ω as explained before. If $\delta > 0$, the sun can be north of the east-west line.

In addition to the angles mentioned in the above equations, it is important to know when it is sunrise or sunset, and calculate its accompanying angles, so that the actuator may be instructed about periods of idleness or activity. For this the following angles and hours are defined.

c) Hour angle at sunrise (ω_{sr}) and sunset (ω_{ss})

At sunrise, the zenith angle is 90o (altitude angle equals to 0o) on a horizontal plane, and this information is used in Equation 7 to obtain the expression for the hour angles at sunrise and sunset. Thus Sunrise (or sunset) hour angle can be calculated from (Tiwari, 2002):

$$\omega_s = \cos^{-1}(-\tan\phi\tan\delta) \quad (9)$$

The sunrise (or sunset) angle can also be evaluated using the following equations (Myer, 2013):

$$\cos\omega_s = \frac{\cos\theta_z - \sin\delta\sin\phi}{\cos\delta\cos\phi} \quad (10)$$

$$\sin\omega_s = -\frac{\cos\alpha\sin\gamma}{\cos\delta} \quad (11)$$

The hour angles at sunrise (ω_{sr}) and sunset (ω_{ss}) are the same numerically (i.e. $|\omega_{sr}| = |\omega_{sr}| = \omega_s$), however the sunrise hour angle is negative and the sunset hour angle is positive.

d) Number of daylight hours (N)

The total angle between sunrise and sunset, in degrees is thus equal to $2\omega_s$. This angle between sunrise and sunset ($2\omega_s$) can be used to find the number of daylight hours (N) for a particular day by using the expression (Tiwari, 2002):

$$N = \frac{2\omega_s}{15} \quad (12)$$

There are always 4380 hours of daylight per year (non-leap year) everywhere on the globe. When $(-\tan\delta\tan\phi) \geq 1$, there is no sunrise (i.e. 24 hours of darkness). This implies that $\omega_{sr} = 0$. Also the solar times at sunrise and sunset for this condition are both equal to 12. When $(-\tan\delta\tan\phi) \leq -1$, there is no sunset (i.e. 24 hours of daylight). This implies that $\omega_{sr} = -180$ and $\omega_{ss} = 180$. The solar times at sunrise and sunset for this condition are respectively equal to 0 and 24.

2.2.3 Optimum set point path for solar Tracking.

Equation (1) shows that in order to make a flat payload track the sun, only its surface orientation (β) and surface azimuth angle (γ) are open to adjustments. The others (the latitude, the declination and the hour angles) are automatically determined from knowledge of the location and the date and time. Therefore, the cosine of the angle of incidence may be expressed as a function of two variables by re-writing Equation (1) as:

$$\cos\theta_i = c_1\cos\beta + c_2\sin\beta\cos\gamma + c_3\sin\beta\sin\gamma \qquad (13)$$

where

$c_1 = \sin\delta\sin\phi + \cos\delta\cos\phi\cos\omega$

$c_2 = \cos\delta\sin\phi\cos\omega - \sin\delta\cos\phi$

$c_3 = \cos\delta\sin\omega$

From Equation (13), the pair of the values of β and γ which makes the cosine of the angle of incidence equal to unity, or the angle of incidence equal to zero, at any location and for specified date and time, is that which makes the payload perfectly tracks the sun at that time. So, sun tracking is about finding the optimum values of this pair at desired times.

Equation (13) can further be reduced to one of a function of a single variable if, at any location and for specified date and time, the payload is oriented such that its surface azimuth angle (γ) is numerically equal to the solar azimuth angle (γ_s), as can be seen from Figures 4 and 5. So Equation (13) may be re-written for case the of perfectly tracked sun as:

$$c_6\cos\beta + c_7\sin\beta - 1 = 0 \qquad (14)$$

where

$c_6 = \sin\delta\sin\phi + \cos\delta\cos\phi\cos\omega$

$c_7 = \cos\delta\sin\phi\cos\omega\cos\gamma_s + \cos\delta\sin\omega\sin\gamma_s - \sin\delta\cos\phi\cos\gamma_s$

With reference to Figure 3, a microcontroller in a pseudo closed loop control can be coded to calculate the desired inclination angle (β) and azimuth angle (γ) a location at regular time intervals in a day, or even as once in a day, once in a month or once a year calculation. Then this optimum data set would be sent to the actuator for the desired altitude and azimuth alignment. The feedback path in the figure (with its sensors or transducers) is optional, just to provide either historical data and/or to provide information about the correctness of the control system.

Optimum value of β for known γ_s, at any location and period, can be evaluated from Equation (14) by closed-domain method for solving nonlinear equations such as bisection method or false position method. The MATLAB® software has a function fminbnd for solving single variable closed-domain problems. Using MATLAB® software, the codes for evaluating Equation (13), and all the associated equations from Equations 1 to 12, are implemented and the trends of the angle of incidence for a range of surface orientation (β) and surface azimuth angle (γ), for Kano, Nigeria (11.9683 °N, 8.4261 °E) at 14:27 hour on 19-OCT-2018, as an example, computed.

2.2.4 Development of the signal flow plan for the pseudo-closed loop solar tracking system

A signal flow plan, which describes an option of calculating the optimum angles for sun tracking as once a day, was developed. A flowchart for implementing such code for a microcontroller was also developed. The option of once a day calculation was preferred over periodic calculations within a day to reduce the computational load on the microcontroller. It was also preferred to the other options (once a month or year calculations) for data storage issues. The proposed pseudo-closed loop solar tracking system would operate by having its set-points (optimum azimuth and slope angle) being automatically adjusted. The development of the signal flow plan for the system is such that it should be fully operational for all days of the year, if it is powered on. The complete signal flow chart is given in Figure 5, and the steps in the signal flow plan are outlined as follows:

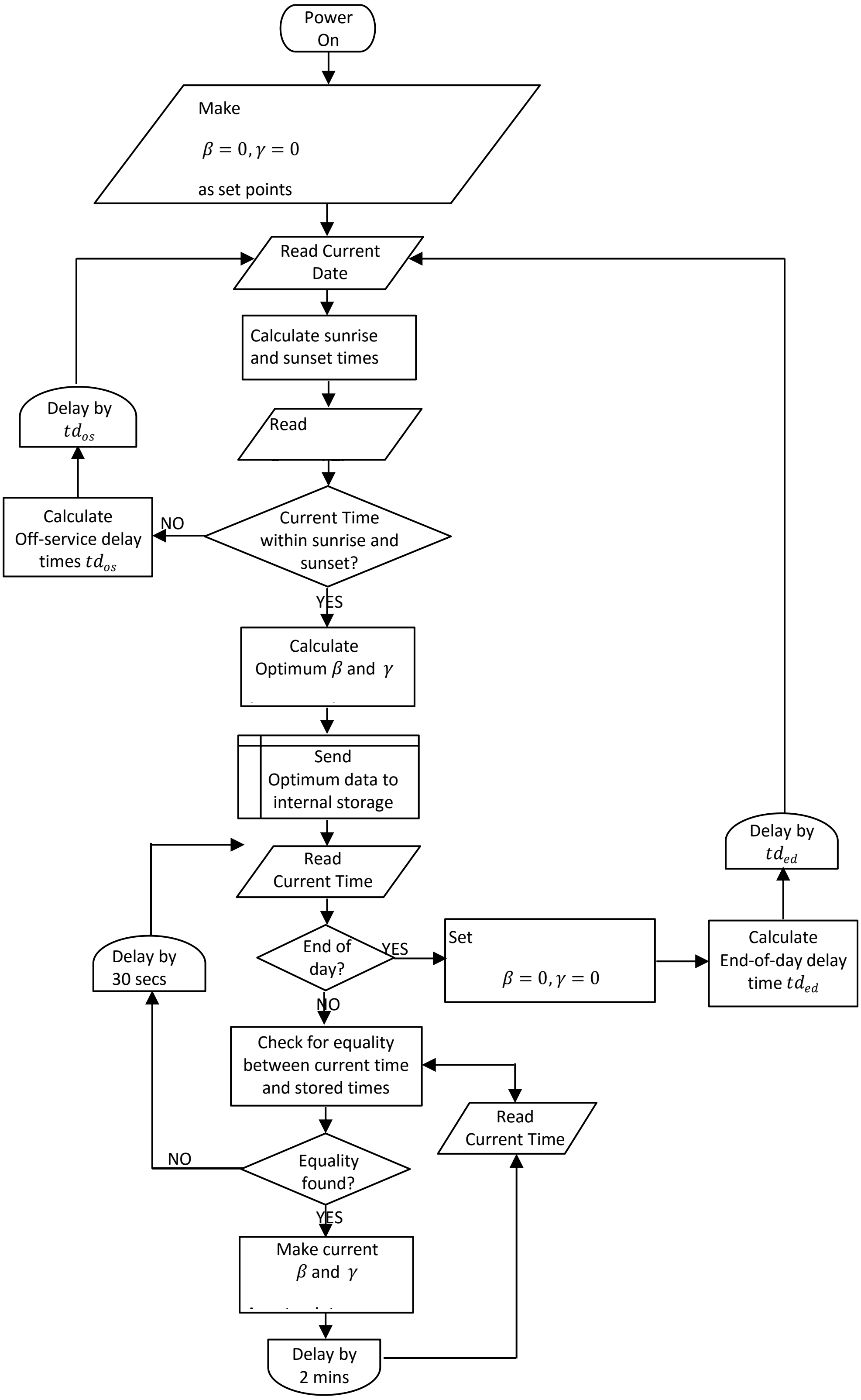

Figure 5: Flow chart for the pseudo-closed loop sun tracking system

At power on, the system reads the latitude and longitude data for the location. It then makes the set-points for the system (azimuth and slope angles) equal to zero.

The system then reads the current date from the attached real time clock

The system then calculates the sunrise and sunset times for the day, using Equations 2,3 and 9.

The system then reads the current time

The system then checks if the current time is within sunrise and sunset times calculated in step 3.

If the current time IS NOT within sunrise and sunset times, the system calculates the necessary delay time td_{os} based on the current time and the sunrise and sunset values calculated. The system is then delayed by td_{os}, then returns to step 3 to attempt another date reading.

If the current time IS within sunrise and sunset times, the system calculates the optimum azimuth and slope angles for specified time intervals (say every 4 minutes) between sunrise and sunset. It uses Equations 2-6, 8, 14

The system sends the optimum set-point data to the internal storage of the microcontroller.

The system reads the current time again (to compensate for any time lapse since the first reading)

The system checks if the end of day has been reached (i.e. if current time is beyond the sunset time value already calculated.

If IT IS end of day, the system calculates the necessary delay time td_{ed} based on the current time and the sunset values calculated. The system is then delayed by td_{ed}, then returns to step 3 to attempt another date reading.

If IT IS NOT end of day, the system searches for a match between the current time and the stored times in the optimum data table of the microcontroller.

If equality IS NOT found in step 11, the system delays by 30 seconds and return to step 8 to read the current time.

If equality IS found, the system sets the corresponding slope and azimuth data that is a match for the data (in step 11) as the set point for the system.

The system delays by 2 minutes (assuming the optimum times were calculated at 4-minute intervals) before returning to step 9.

3. Results and Discussions

As an example, the plots of the trends of the incident angles (θ_i) for various azimuth angles (γ) and inclination angles (β) are plotted as shown in Figure 6 for Kano, Nigeria (11.9683 °N, 8.4261 °E) at 14:27 hour on 19-OCT-2018. While Figure 6(a) shows the 3-D plot, Figure 6b shows its contour plot. The contour plot (with the colour bar at the right) shows that at this time, the optimum pair of β and γ lie in the darkest part of the plot (the dark blue region is the region of lowest angle of incidence), which evaluates to between 22° to 55° for β and 30° to 75° for γ.

While Figure 6 shows the different combinations of azimuth angles (γ) and inclination angles (β) to give possible incident angles (θ_i) at an instant (a given time), Figure 7 shows the plots of optimum pairs of β and γ for a day. For the date specified for Kano, Nigeria on 19-OCT-2018, the optimum pair of β and γ that will make a flat payload track the sun from sunrise to sunset are given in the figure. The solar time is shown on the horizontal axis while the azimuth and inclination angles are shown on the vertical axes. For example, the figure shows that the optimum pair of β and γ at 10.00 solar time on this date is about 55° for β and -40° for γ (the points where β and γ curves intersect the 10.00 solar time line). Likewise on this date, the optimum pair of β and γ at 12.00 solar time is about 0o for β and 35° for γ, and at 14.00 solar time, the optimum pair is about 45° for β and 40° for γ.

4.0 Conclusions

A concept of pseudo-closed loop solar tracking system for a flat payload, where the set-points for the system are optimally computed by a microcontroller, and the outputs of the system (the slope and the azimuth angles of the payload) observed, has been proposed. The models for the development of the optimum set point path for the tracking system for use within a microcontroller are also presented. Example of using the models to calculate optimum payload orientation angle and azimuth angle for a given day was presented. The outline of the signal flow plan for the tracking system's component interaction, and the corresponding flowchart, were also developed and presented. The pseudo-closed loop solar tracking system offers a viable and cheaper alternative to a full closed loop solar tracking system.

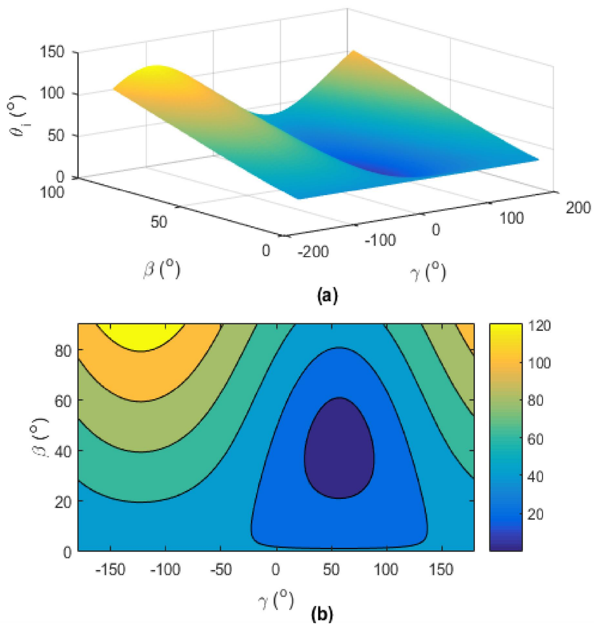

Figure 6: 3-D plot (a) and contour plot (b) of angles of incidence for ranges of inclination angle (β) and azimuth angle (γ) for Kano, Nigeria (11.9683 °N, 8.4261 °E) at 14:27 hour on 19-OCT-2018

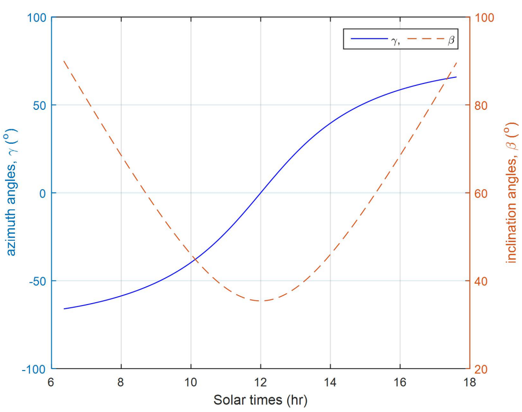

Figure 7: Plots of optimum pairs of inclination angle (β) and azimuth angle (γ) from sunrise to sunset for Kano, Nigeria (11.9683 °N, 8.4261 °E) on 19-OCT-2018

Reference

Abdallah, S. and Nijmeh, S. 2004. Two axes sun tracking system with PLC control. Energy Conversion and Management , 45: 1931-1939.

Aiuchi, K., Yoshida, K., Katayama, Y., Nakamura, M. and Nakamura, K. 2004. Sun tracking photo-sensor for solar thermal concentrating system. In: Proceedings of International Solar Energy Conference. Portland, USA. July 11- 14, 2004

Alata, M., Al-Nimr, M. and Qaroush, Y. 2005. Developing a multipurpose sun tracking system using fuzzy control. Energy Conversion and Management, 46: 1229-1245.

Al-Naima, F. and Yaghobian, N. 1990. Design and construction of a solar tracking system. Solar Wind Technology, 7: 611-617.

Bari, S. 2000. Optimum slope angle and orientation of solar collectors for different periods of possible utilization. Energy Conversion and Management, 41: 855-860.

Barsoum, N. 2011. Fabrication of Dual-Axis Solar Tracking Controller Project. Intelligent Control and Automation, 2: 57- 68.

Blanco-Muriel, M., Alarcón-Padilla, D., López-Moratalla, T. and Lara-Coira, M. 2001. Computing the Solar Vector. Solar Energy, 70(5): 431-441.

Duffie, JA. and Beckman, WA. 1991. Solar Energy Thermal Processes. New York: John-Wiley and Sons., pp 45.

Georgiev, A., Roth, P. and Olivares, A. 2004. Sun following system adjustment at the UTFSM. Energy Conversion and Management, 45: 1795-1806.

Grena, R. 2008. An algorithm for the computation of the solar position.. Solar Energy, 82: 462-470.

IEA 2018. International Energy Agency, Renewables 2018 Market analysis and forecast from 2018 to 2023. [Online] Available at: https://www.iea.org/renewables2018/. [Accessed 28 Jan 2019].

Iqbal, M. 1983. An Introduction to Solar Radiation. New York: Academic Press.

Jiang, W. and Cao, M. 2003. Emulation sunflower. In: Proceedings of the International Symposium on Test and Measurement. Shenzhen, China: June 1-5. 2003.

Kalogirou, S. 1996. Design and construction of a one-axis sun-tracking system. Solar Energy, 57: 465-469.

Lee, C., Chou, P., Chiang, C. and Lin, C. (2009). Sun Tracking Systems: A Review.. Sensors , 9: 3875-3890.

Meeus, J. 1998. Astronomical Algorithms. Second edition ed. Virginia, USA: Willmann-Bell, Inc., Richmond. pp 77

Michalsky, JJ. 1988. The asreonomical almanac’s algorithm for approximate solar position (1950-2050). Solar Energy., 40(3): 227-235.

Mohd, H., Yakup, M. and Malik, A. 2001. Optimum tilt angle and orientation for solar collector in Brunei Darussalam. Renewable Energy, 24: 223-234.

Myer, DR. 2013. Solar Radiation Practical Modeling for Renewable Energy Applications. London: CRC Press., pp 102.

NASA 2018. Scientific consensus: Earth's climate is warming. [Online] Available at: https://climate.nasa.gov/scientific-consensus/ [Accessed 2019].

Reda, I. and Andreas, A. 2004. Solar position algorithm for solar radiation applications.. Solar Energy, 76: 577-589.

Roth, P., Georgieg, A. and Boudinov, H. 2004. Design and construction of a system for sun-tracking. Renewable Energy, 29: 393-402.

Simonson, JR. 1984. Computing Methods in Solar Heating Design. London: Macmillan Press., pp 10.

Spencer, J. W. 1971. Fourier series representation of the position of the sun. Search,. 2: 162-172.

Tiwari, N. 2002. Solar Energy: Fundamentals, Design, Modelling and applications.. India: Narosa publishing., pp 7.

Xinhonz, Z., Zongxian, W. and Zhengda, Y. 2007. Intelligent Solar tracking Control System Implemented on an FPGA. NiOS II Embedded Process Design Contest – Outstanding Design 2007, pp 217 – 245. [Online]. Available at: https://www.intel.com/content/dam/www/programmable/us/en/pdfs/literature/dc/_2007/t3c.pdf [Accessed 2019]